Molecular Cancer

RESEARCH Open Access

CircLIFRSA/miR-1305/PTEN axis attenuates malignant cellular processes in non-small cell lung cancer by regulating AKT phosphorylation

Meina Jiang[1], Huihui Bai[1], Shuai Fang[1], Chengwei Zhou[2], Weiyu Shen[3] and Zhaohui Gong[1,2*]

Abstract

Background Non-small cell lung cancer (NSCLC) is typically diagnosed at advanced stages, which limits the effectiveness of therapeutic interventions. The present study aimed to explore the role of the newly identified circLIFRSA in the PTEN/AKT signaling pathway and its involvement in the malignant processes of NSCLC.

Methods CircLIFRSA expression was identified through microarray analysis, and its levels in NSCLC samples were quantified by RT-qPCR. The impact of circLIFRSA on cell growth, proliferation, apoptosis, and cell cycle were evaluated by MTT assay, colony formation assay, and flow cytometry. Additionally, Western blotting was employed to analyze the expression of PTEN and phosphorylated AKT (pAKT) in NSCLC cells.

Results The expression of circLIFRSA was found to be significantly reduced in NSCLC cells and tissues. This downregulation correlated with various clinicopathological characteristics and indicated its potential as an early diagnostic biomarker for NSCLC. Importantly, circLIFRSA was shown to inhibit cell growth and proliferation while promoting apoptosis in NSCLC cells. Mechanically, circLIFRSA was found to attenuate the malignant processes of NSCLC cells via the miR-1305/PTEN axis and the suppression of AKT phosphorylation.

Conclusions These findings indicate that circLIFRSA/miR-1305/PTEN axis attenuates malignant processes by regulating AKT phosphorylation, and provide new insights into the potential of circLIFRSA as a biomarker for early diagnosis and as a promising therapeutic target in NSCLC.

Keywords Circular RNA, LIFRSA, Malignant process, miR-1305, Non-small cell lung cancer, AKT phosphorylation

*Correspondence:
Zhaohui Gong
gongzhaohui@nbu.edu.cn
[1]Department of Biochemistry and Molecular Biology and Zhejiang Key Laboratory of Pathophysiology, School of Basic Medical Sciences, Health Science Center, Ningbo University, Ningbo, Zhejiang 315211, China
[2]Department of Thoracic Surgery, The First Affiliated Hospital of Ningbo University, Ningbo, Zhejiang 315020, China
[3]Department of Thoracic Surgery, The Affiliated Lihuili Hospital of Ningbo University, Ningbo, Zhejiang 315040, China

Background

Lung cancer is recognized as the leading cause of cancer-related fatalities worldwide, significantly contributing to mortality rates among both male and female populations [1]. Given the considerable diversity in clinical and pathological characteristics, lung cancer can be broadly categorized into two primary types: non-small cell lung cancer (NSCLC) and small cell lung cancer (SCLC). NSCLC accounts for approximately 85% of all lung cancer cases, making it the most prevalent subtype [2]. Although there has been a gradual decrease in the incidence of advanced lung cancer over recent decades, the annual rate of early-stage lung cancer diagnoses has increased by 4.5% [3]. Currently, the 3-year survival rate for lung cancer patients remains below 35% [1]. The mechanisms underlying the pathogenesis of lung cancer, particularly NSCLC, are not fully understood. Consequently, it is essential to investigate the molecular mechanisms that contribute to the initiation and progression of NSCLC. Such research may provide valuable insights into the identification of biomarkers and the development of novel therapeutic agents.

Circular RNAs (circRNAs) represent a distinct class of noncoding RNAs (ncRNAs) characterized by their covalently closed, continuous loop structures. Research has identified differentially expressed circRNAs that are implicated in the initiation and progression of various cancer types [4, 5]. Due to their unique structure properties, circRNAs are often recognized for their role as endogenous competing RNAs (ceRNAs), which are integral to the regulation of gene expression [6–12]. For example, circPTK2 has been shown to function as a ceRNA for transcriptional intermediary factor 1 gamma (TIF1γ) by sponging miR-429 and miR-200b-3p, thereby inhibiting TGF-β-induced epithelial-mesenchymal transition (EMT) and tumor metastasis in NSCLC. This suggests that overexpression of circPTK2 may represent a potential therapeutic strategy for advanced NSCLC [13]. However, the functions and mechanisms of newly identified circRNAs in NSCLC remain largely unexplored. The aberrant activation of the phosphoinositide 3-kinase (PI3K)/AKT signaling cascade has been widely observed and is known to play a significant role in various cancer hallmarks, including cell growth, metabolism, and metastasis [14, 15]. In esophageal squamous cell carcinoma (ESCC), circLPAR3 has been shown to enhance cell migration, invasion, and metastasis by regulating the miR-198-MET signaling axis and activating the RAS/MAPK and PI3K/AKT pathways [16]. Additionally, circVRK1 has been reported to inhibit the progression of ESCC by modulating the miR-624-3p/PTEN axis and the PI3K/AKT signaling pathway [17]. In the context of NSCLC, the frequent loss of PTEN, an antagonist of the PI3K/AKT pathway, is a common event that contributes to oncogenic transformation [18]. Nonetheless, it remains to be determined whether newly discovered circRNAs are invovled in the PTEN/AKT pathway and whether they contribute to the malignant progression of NSCLC.

In the present study, we discovered a novel circRNA, hsa_circ_0072298, designated as circLIFRSA, which exhibited diminished expression levels in both NSCLC cells and tissues. Additionally, the downregulation of circLIFRSA showed a significant correlation with various clinicopathological characteristics, suggesting its potential as a promising biomarker for distinguishing benign lung conditions, and early-stage NSCLC from lung cancer. Notably, circLIFRSA was found to inhibit cell growth and proliferation while promoting apoptosis in NSCLC. Mechanically, circLIFRSA was shown to attenuate malignant processes via the miR-1305/PTEN axis, leading to the suppression of AKT phosphorylation. These results indicate that circLIFRSA may serve as a new biomarker for early diagnosis and as a novel therapeutic target for patients with NSCLC.

Materials and methods

Clinical specimens

A total of 101 lung cancer tissues and corresponding para-carcinoma tissues were obtained from the First Affiliated Hospital of Ningbo University (Ningbo, China) and the Affiliated Lihuili Hospital of Ningbo University (Ningbo, China). These tissue specimens were utilized for further various analyses (Additional file 1, Figure S1). Additionally, whole blood samples were collected from 49 healthy individuals, 30 patients with benign lung diseases, and 60 patients diagnosed with lung cancer from the aforementioned hospitals. These blood samples were employed for the assessment of circLIFRSA expression and receiver operating characteristic (ROC) analysis (Additional file 1, Figure S2). The patients with primary lung cancer included in this study had not received preoperative chemotherapy, and their clinical data were collected and subsequently analyzed. The study was approved by the Medical Research Ethics Committee of Ningbo University (Approval No.: NBU-2021-032), and all participants provided written informed consent.

Cell culture and transfection

Human lung adenocarcinoma cell lines (A549, NCI-H1299), as well as normal human bronchial epithelial cells (HBE), were maintained in RPMI-1640 medium (Hyclone, USA) supplemented with 10% fetal bovine serum (FBS) (PAN, Germany) under conditions of 37 °C and 5% CO_2. Transfections were performed using either circLIFRSA siRNA (GenePharma, China) alongside its corresponding negative control RNA (siRNA NC), or a recombinant plasmid designed to overexpress

circLIFRSA in conjunction with the empty pcDNA3.1(+) circRNA Mini vector (Addgene, USA). Furthermore, miR-1305 mimics (GenePharma, China) along with their corresponding control RNA (miR-NC) were introduced into the cells using lipofectamine 2000 (Invitrogen, USA), following the manufacturer's protocols. The sequences for miR-1305 mimics and siRNA oligonucleotides are shown in Additional file 2, Table S1.

RT-qPCR

RNA isolation was performed on lung cancer tissues, blood samples, and cell lines utilizing Trizol reagent (Invitrogen, USA) following the recommended manufacturer's protocols. Subsequently, cDNA synthesis was carried out with the NovoScript® Plus All-in-one 1st Strand cDNA Synthesis SuperMix (gDNA Purge) kit (Novoprotein, China) and Hairpin-itTM miRNAs RT-PCR Quantitation Kit (GenePharma, China). Quantitative PCR (qPCR) was conducted using the NovoScript® SYBR qPCR SuperMix Plus kit (Novoprotein, China) on an Mx3005P real-time PCR System (Stratagene, USA), following the manufacturer's instructions. The quantification of circLIFRSA in whole blood using absolute plasmid DNA standards as described previously [19]. Primer sequences are detailed in Additional file 2, Table S2.

Plasmid construction

The gene sequence of circLIFRSA was amplified by PCR from the cDNA of the HBE cell line and subsequently subcloned into either the pcDNA3.1(+) CircRNA Mini Vector (LMAI Bio, China) or the pGL3-control vector (Promega, USA) as described in our previous work [20].

MTT assay

Cells were plated at a density of 3×10^3 cells per well in 200 μL of media within 96-well plates and incubated for 24 h until they reached 50–60% confluency. Following this, transfection with the plasmid overexpressing circLIFRSA was performed, and the cells were cultured for an additional culture period ranging from 24 to 96 h. At specified time points post-transfection (24, 48, 72, and 96 h), 20 μL of MTT (Solarbio, China) was added to each well and incubated for 4 h. Subsequently, the media were aspirated, and 150 μL of DMSO was gently added to each well. The absorbance was quantified by measuring the optical density (OD) values at 490 nm using a microplate reader (Labsystems, Finland).

Colony formation assay

In a 6-well plate, each well was initially seeded with 1500 cells and incubated for 24 h. Following this incubation, cells were transfected with the plasmid overexpressing circLIFRSA. The culture medium was refreshed after one week, with subsequent changes occurring every three days for a two-week period. Upon completion of the cultivation phase, the cells were washed twice with PBS, fixed in 4% paraformaldehyde (Solarbio, China) for 30 min, and subsequently stained with 0.1% crystal violet (Solarbio, China) for an additional 30 min. Colony counting in each well was performed using a microscope (Olympus, Japan).

Cell apoptosis assay

The culture supernatant from the 6-well plate was collected, and the cells were subjected to two washes with PBS. Following this, the cells were trypsinized using trypsin without EDTA, and the trypsin activity was neutralized by the addition of the previously collected supernatant. The cell suspension was then centrifuged at 1000 rpm for 8 min. The subsequent procedures involved additional washing with PBS, resuspension in the Binding Buffer (BD Pharmingen, USA), and incubation in the dark at room temperature for 20 to 30 min. Finally, flow cytometry analysis (Beckman, USA) was conducted on the prepared cell samples.

Cell cycle assay

Cells (2×10^5 per well) were cultured in 6-well plates and starved for 24 h to reach approximately 60% confluence. Subsequently, transfection was performed with the plasmid overexpressing circLIFRSA, followed by an additional 48 h of culture. The cells were then suspended in 70% ethanol and incubated at −20 °C for 24 h. After centrifugation at 3000 rpm at 4 °C for 5 min, the ethanol was removed, and the cell pellet was washed with PBS. The pellet was then resuspended in 1 mL of cold PBS containing 100 μg/mL RNase and incubated at 37 °C for 2 h. Following another centrifugation, 200 μL of DNA staining solution (BD Pharmingen, USA) was added, and flow cytometry analysis (Beckman, USA) was employed to evaluate the distribution of the cell cycle.

CircRNA localization analysis

Nuclear and cytoplasmic fractions from lung cancer cells were obtained using the PARISTM Kit (Thermo Fisher Scientific, USA). Subsequently, RT-qPCR was employed to separately evaluate the expression levels of circLIFRSA and internal controls (GAPDH, U6) within these distinct cellular compartments.

RNA stability assay

Cells were treated with 5 μg/mL Actinomycin D (Selleck, China) and subsequently harvested at predetermined time intervals. The turnover rate and half-life of circLIFRSA and mLIFRSA were assessed utilizing a previously established protocol [21].

Dual-luciferase reporter assay

Recombinant dual-luciferase reporter vectors were generated by subcloning the core sequences of circLIFRSA, PTEN wild-type/mutant-type, and miR-1305 into their corresponding reporter vectors. Co-transfection of these constructs along with miR-1305 mimics was performed in NSCLC cells. The resulting luciferase activity was measured using the dual-luciferase reporter system (Promega, USA).

Western blotting

Cellular proteins were extracted by harvesting cells and lysing them in RIPA buffer (Solarbio, China). The BCA Protein Assay kit (Beyotime, China) was employed to quantify the cellular protein content. Subsequently, 30 μg of protein samples were separated on 10% SDS-PAGE and transferred onto a PVDF membrane via a wet transfer apparatus (Bio-Rad, USA) for 1 h. Following a blocking step with 5% BSA at room temperature for 1 h, the membrane was incubated overnight at 4 °C with primary antibodies against PTEN (1:1000, sc-7974, Santa Cruz Biotechnology, USA), tAKT (1:1000, sc-81434, Santa Cruz Biotechnology, USA), pAKT (1:1000, sc-514032, Santa Cruz Biotechnology, USA), or GAPDH (1:1000, sc-47724, Santa Cruz Biotechnology, USA). Subsequently, the membranes were washed three times with TBST buffer (10 min each) and incubated with an HRP-labeled secondary antibody (ABconal, China) for 1 h at room temperature. After additional washing, signals were detected using an enhanced chemiluminescence (ECL) kit (Beyotime, China), and the relative expression of each protein was quantified using Image J software (NIH, USA).

Statistical analysis

Statistical analyses were performed using GraphPad Prism 8 software (GraphPad Software, USA). Each experiment was conducted in triplicate, and the results are presented as the mean ± SD from three independent trials. The chi-square test was utilized to assess the correlation between circLIFRSA expression and clinical characteristics in lung cancer patients. Student's t-test, one-way ANOVA, and Pearson correlation analysis were utilized for mean comparisons between groups. A significance threshold of $P<0.05$ was applied to determine statistical significance across all analyses.

Results

CircLIFRSA is a new circular RNA with stable loop structure

To identify circRNAs associated with lung cancer, we conducted an analysis of circRNA expression profiles in cancer tissues and para-carcinoma tissues from lung cancer patients, utilizing microarray analysis (GSE126533). Our investigation revealed a total of 7,081 differentially expressed circRNAs, comprising 3,924 that were downregulated and 3,157 that were upregulated (Fig. 1A). From these, the top 100 circRNAs exhibiting significant aberrant expression were selected for further examination (Fig. 1B). To maintain a degree of novelty, certain previously reported circRNAs were excluded based on a thorough literature review. Given the relationship between parental gene information and tumorigenesis, hsa_circ_0072298 was identified as significantly downregulated and was subsequently chosen for further study (Fig. 1A). Hsa_circ_0072298 is derived from the leukemia inhibitory factor receptor subunit alpha (LIFRSA) gene, which produces 12 circular transcripts through alternative splicing. According to circRNA sequencing data (GSE152434), hsa_circ_0072298 was found to be the most abundant among the 12 circRNAs generated by LIFRSA (Fig. 1C). Furthermore, circLIFRSA (hsa_circ_0072298) exhibited higher expression levels in normal human lung epithelial cells compared to human lung cancer cell lines, corroborating its downregulation observed in tissue microarray analysis. As a result, circLIFRSA was selected for further exploration of its functional role and underlying mechanism in lung cancer progression.

To validate the stability of loop circLIFRSA, we compared it with its homologous linear counterpart, LIFRSA mRNA (mLIFRSA), using divergent primer RT-qPCR and actinomycin D treatment. CircLIFRSA, which is located on chromosome 5 and spans 2,689 nucleotides, was analyzed using divergent primers designed to amplify a fragment containing the back junction site of circLIFRSA, while convergent primers were employed to amplify a partial fragment of mLIFRSA (Fig. 1D). The results demonstrated that the divergent primers did not yield a product when applied to genomic DNA (gDNA) but successfully amplified a product containing the back junction site from complementary DNA (cDNA), thereby confirming the loop structure of circLIFRSA (Fig. 1E). Additionally, the actinomycin D-mediated gene transcription inhibition assay revealed that the half-life of circLIFRSA was significantly longer than that of mLIFRSA (Fig. 1F). The findings substantiate that circLIFRSA, characterized by its loop structure, exhibits enhanced stability in comparison to the linear transcript mLIFRSA.

CircLIFRSA is downregulated and associated with various clinicopathological characteristics in NSCLC

To assess the expression levels of circLIFRSA in NSCLC, RT-qPCR was employed to evaluate its baseline expression in normal human bronchial epithelial (HBE) cells, NSCLC cell lines, and tumor tissues. The results revealed a significant downregulation of circLIFRSA in NSCLC cell lines when compared to normal HBE cells (Fig. 2A). The predominance of circLIFRSA in the cytoplasm of

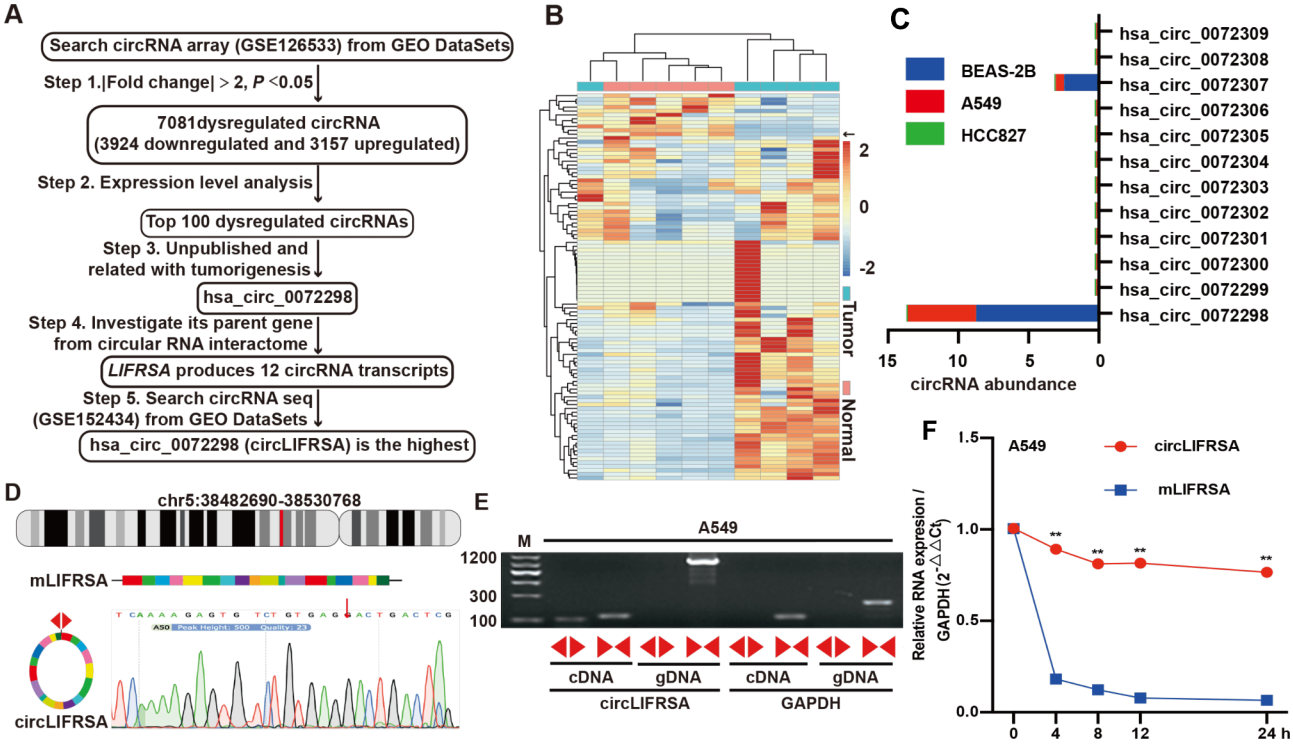

Fig. 1 CircLIFRSA is a new circular RNA with stable loop structure. (**A**) Workflow of screening hsa_circ_0072298. (**B**) Heatmap of top 100 dysregulated circRNAs. (**C**) Prediction of the abundance of all circRNA transcripts generated from LIFRSA via circular RNA interactome (step 4 in Fig. 1A). (**D**) Origin of linear mLIFRSA and circular circLIFRSA. Arrows indicate the back junction site. (**E**) Agarose gel electrophoresis of circLIFRSA amplified by PCR in A549 cells. Divergent primers can amplify circLIFRSA in cDNA but not in genomic DNA (gDNA). GAPDH was used as a negative control. (**F**) The relative RNA levels of circLIFRSA and mLIFRSA were analyzed by RT-qPCR after treatment with actinomycin D at the indicated time points in A549. The half-life of circLIFRSA is longer than that of mLIFRSA. ** $P < 0.01$

NSCLC cells was confirmed through nuclear and cytoplasmic RNA fractionation, which demonstrated over 70% cytoplasmic localization (Fig. 2B). In patients with NSCLC, circLIFRSA expression was significantly lower in tumor tissues compared to adjacent para-carcinoma tissues (Fig. 2C-E). Among the 101 cases analyzed, 9 cases (8.9%) exhibited upregulation, 13 cases (12.9%) showed no significant change, and 79 cases (78.2%) were downregulated (Fig. 2F). These results suggest that circLIFRSA is expressed at low levels in NSCLC cells and tissues.

To further investigate the relationship between reduced circLIFRSA expression and clinicopathological characteristics, comprehensive clinicopathological data from 74 lung cancer patients were collected, and a chi-square analysis was perfomed. The analysis revealed that circLIFRSA expression did not correlate with age (P=0.1083), gender (P=0.1067), lesion location (P=0.3074), body mass index (BMI) (P=0.0833), smoking history (P=0.7899), metastasis (P=0.7115), TNM stage (P=0.0564), CYFRA21-1 (P=0.12), CA199 (P=0.3511), or CA125 (P=0.3575). However, decreased circLIFRSA expression was significantly associated with tumor size (P=0.0381), the number of tumors (P=0.0438), differentiation grade (P=0.005), and pathological type (P=0.0144) (Table 1). These findings suggest the potential clinical relevance of circLIFRSA in the context of NSCLC.

Blood-derived circLIFRSA serves as an early diagnostic biomarker for lung cancer

To evaluate the diagnostic performance of circLIFRSA, we utilized RT-qPCR to quantify its expression levels in whole blood samples from three groups: healthy individuals (n=49), individuals with benign lung diseases (n=30), and patients diagnosed with lung cancer (n=60). The demographics of the healthy controls and patients with benign lung disease did not show significant correlations with age (P=0.4115), gender (P=0.1738), BMI (P=0.0965), or smoking status (P=0.2839) (Additional file 2, Table S3). Following established methodologies (as referenced in previous work [19]), a standard curve was generated to determine the copies of circLIFRSA in whole blood based on RNA concentration and cycle threshold (Ct) values through gradient dilution (Fig. 3A). Notably, circLIFRSA was detected at minimal levels in the whole blood of healthy individuals. In contrast, there was a slight increase in circLIFRSA copies in the whole blood of patients with benign lung diseases compared

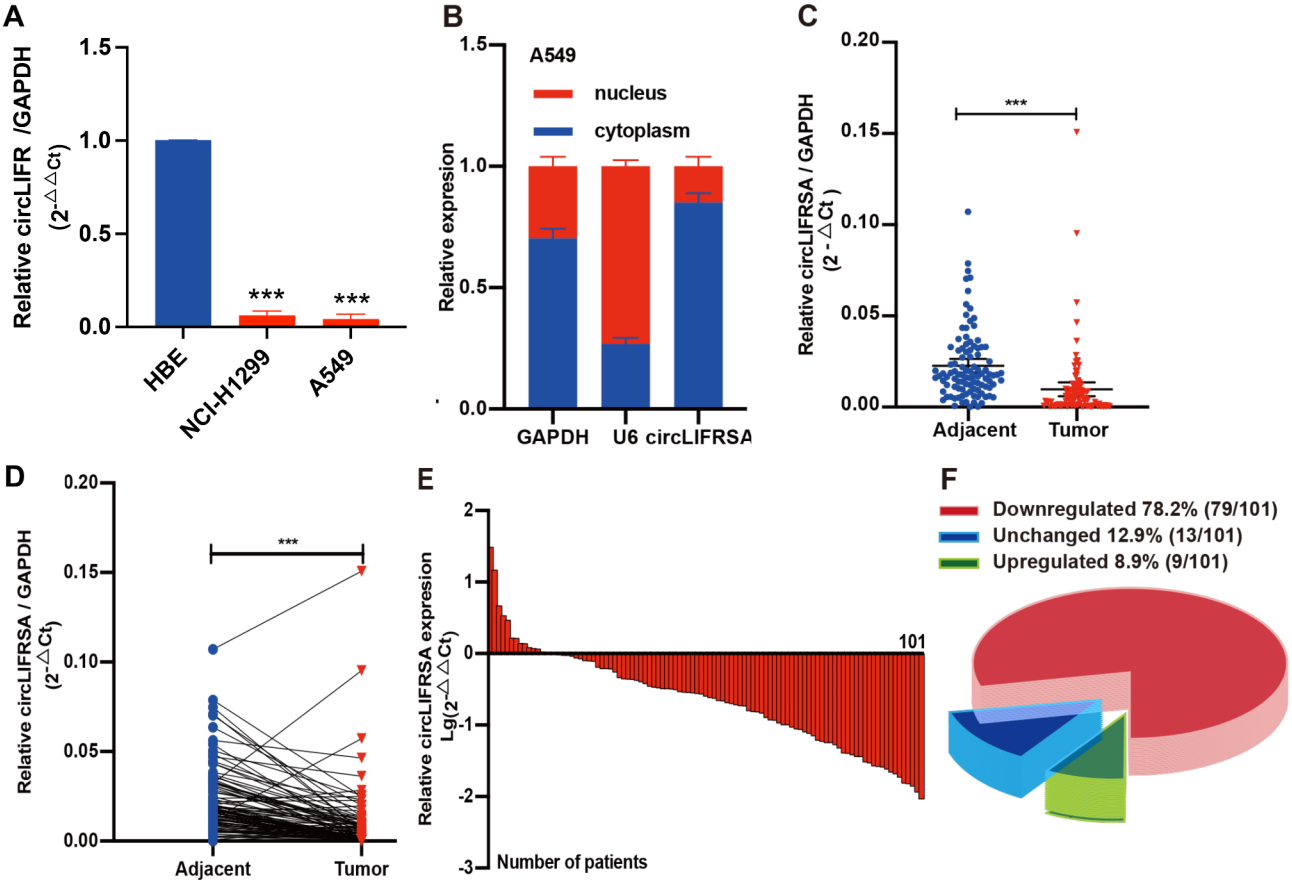

Fig. 2 CircLIFRSA is downregulated in NSCLC cells and tissues, localized in cytoplasm. (**A**) The expression levels of circLIFRSA in NSCLC cells was detected by RT-qPCR. (**B**) The localization of circLIFRSA was determined by nuclear and cytoplasmic RNA fractionation and RT-qPCR analysis. (**C-F**) The expression of circLIFRSA in tumor and adjacent tissues of NSCLC patients was detected by RT-qPCR ($n = 101$). *** $P < 0.001$

to healthy controls. Importantly, patients with lung cancer exhibited an average of approximately 500 copies per microliter of whole blood (Fig. 3B). ROC curve analysis indicated that circLIFRSA achieved an area under the curve (AUC) value of 0.8578 (95% CI: 0.7539–0.9616) for differentiating benign lung diseases from lung cancer, with a sensitivity of 98.53% and specificity of 81.52% (Fig. 3C). Furthermore, the ROC curve analysis demonstrated that circLIFRSA yielded an AUC value of 0.7542 (95% CI: 0.7265–0.9481) for distinguishing early stage I NSCLC from more advanced stages (II-IV), with a sensitivity of 64% and specificity of 82%) (Fig. 3D). Therefore, circLIFRSA has the potential to serve as an early diagnostic biomarker for patients with NSCLC.

CircLIFRSA exerts inhibitory effects on the malignant processes of NSCLC cells

Given the observed association between circLIFRSA and tumor size in NSCLC patients (Table 1), we hypothesized its role in the modulation of cancer cell growth. To explore this hypothesis, we performed a gain-of-function experiment targeting circLIFRSA to evaluate its impact on cell growth and proliferation in A549 cells. The results showed that the efficacy of circLIFRSA overexpression (OE) was approximately 80 times greater than that of the vector control group in A549 cells (Fig. 4A). The MTT assay revealed that the overexpression of circLIFRSA significantly inhibited cell growth in A549 cells (Fig. 4B). In addition, the colony formation assay demonstrated that circLIFRSA overexpression impeded the formation of cell clones in A549 cells (Fig. 4C). These findings suggest that the upregulation of circLIFRSA effectively suppresses cell growth and proliferation. Regarding the effects of circLIFRSA on cell apoptosis and cell cycle progression, our results indicated that circLIFRSA overexpression enhanced apoptosis in A549 cells (Fig. 4D). Nevertheless, it is noteworthy that circLIFRSA overexpression did not significantly influence DNA content or the cell proliferation index (PI) at various stages in A549 cells (Additional file 1, Figure S3). Consequently, while circLIFRSA appears to induce cell apoptosis, it does not appear to affect cell cycle progression in NSCLC.

Table 1 Correlations between circLIFRSA expression and clinical characteristics

Parameters		Expression of circLIFRSA		*P* value
	Cases	High	Low	
Age				0.1083
≤55	11	8	3	
>55	63	28	35	
Gender				0.1067
Male	44	18	26	
Female	30	18	12	
Lesion location				0.3074
Right	49	24	25	
Left	23	10	13	
Bilateral	2	2	0	
BMI				0.0833
<22	36	16	20	
≥22	38	20	18	
Smoking history				0.7899
Yes	32	15	17	
No	42	21	21	
Tumor size(cm)				0.0381*
<2	46	27	19	
≥2	28	9	19	
Numbers of tumor				0.0438*
Solitary	64	28	36	
Multiple	10	8	2	
Metastasis				0.7115
Yes	8	3	5	
No	66	33	33	
TNM stage				0.0564
I/II	66	35	31	
III/IV	8	1	7	
Differentiation grade				0.005**
High	39	25	14	
Low	35	11	24	
Pathological type				0.0144*
Squamous carcinoma	25	7	18	
Adenocarcinoma	45	28	17	
Other type	4	1	3	
Serum CYFRA21-1				0.12
≤3.3	49	27	22	
>3.3	25	9	16	
CA199				0.3511
>35	70	33	37	
≥35	4	3	1	
CA125				0.3575
>35	68	35	33	
≥35	6	1	4	

*$P < 0.05$, ** $P < 0.01$

CircLIFRSA interacts and negatively correlates with miR-1305

Given its predominant localization in the cytoplasm (Fig. 2B), we speculated that circLIFRSA may function as a miRNA sponge. Potential miRNAs associated with circLIFRSA were predicted using bioinformatics tools, including TSCD, circBank, and circular RNA interactome. Venn diagram analysis revealed that miR-1305 is the sole candidate miRNA capable of binding to circLIFRSA (Fig. 5A). This interaction between circLIFRSA and miR-1305 was further validated through dual-luciferase activity assays, which demonstrated binding to core elements (Fig. 5B). Furthermore, miR-1305 was found to be significantly upregulated in NSCLC cells compared to HBE cells (Fig. 5C). Notably, the overexpression of circLIFRSA resulted in a marked downregulation of miR-1305 expression in A549 cells (Fig. 5D). Additionally, elevated levels of miR-1305 were detected in NSCLC tumor tissues in comparison to adjacent tissues (Fig. 5E-G). Among 39 NSCLC cases analysed, 29 cases (74.4%) exhibited upregulation of miR-1305, 1 case (2.5%) showed no change, and 9 cases (23.1%) demonstrated downregulation (Fig. 5H). Moreover, a negative correlation between circLIFRSA and miR-1305 was observed in NSCLC patients (Fig. 5I), indicating an interaction characterized by inverse expression levels.

To further explore the prognostic significance of miR-1305, bioinformatic analysis was performed utilizing the RNA transcriptome database and the Encyclopedia of RNA interactome. The results indicated that miR-1305 expression was elevated in both lung adenocarcinoma (LUAD) and lung squamous cell carcinoma (LUSC) tissues compared to adjacent para-carcinoma tissues (Additional file 1, Figure S4A). Survival curve analysis revealed that LUAD patients with high miR-1305 expression experienced poorer survival outcomes compared to those with low miR-1305 expression ($P<0.05$) (Additional file 1, Figure S4B). However, no significant difference in the overall survival (OS) rate was observed between high and low miR-1305 expression groups among LUSC patients (Additional file 1, Figure S4B). These findings suggest that miR-1305, as an intermediary for circLIFRSA, may serve as a risk factor for the prognosis of LUAD patients.

CircLIFRSA suppresses the malignant processes by regulating miR-1305

To investigate whether the influence of circLIFRSA on cellular phenotypes is mediated by its interaction with miR-1305, co-transfection experiments involving circLIFRSA and miR-1305 were conducted in NSCLC cells. The MTT assay demonstrated that miR-1305 facilitated cell growth, while circLIFRSA attenuated the growth-promoting effect of miR-1305 in A549 cells (Fig. 6A). In terms of cell colony formation, the results indicated that miR-1305 enhanced cell proliferation, whereas circLIFRSA diminished this promoting effect of miR-1305 on cell proliferation (Fig. 6B). Regarding cell apoptosis, flow cytometry analysis revealed that miR-1305 inhibited

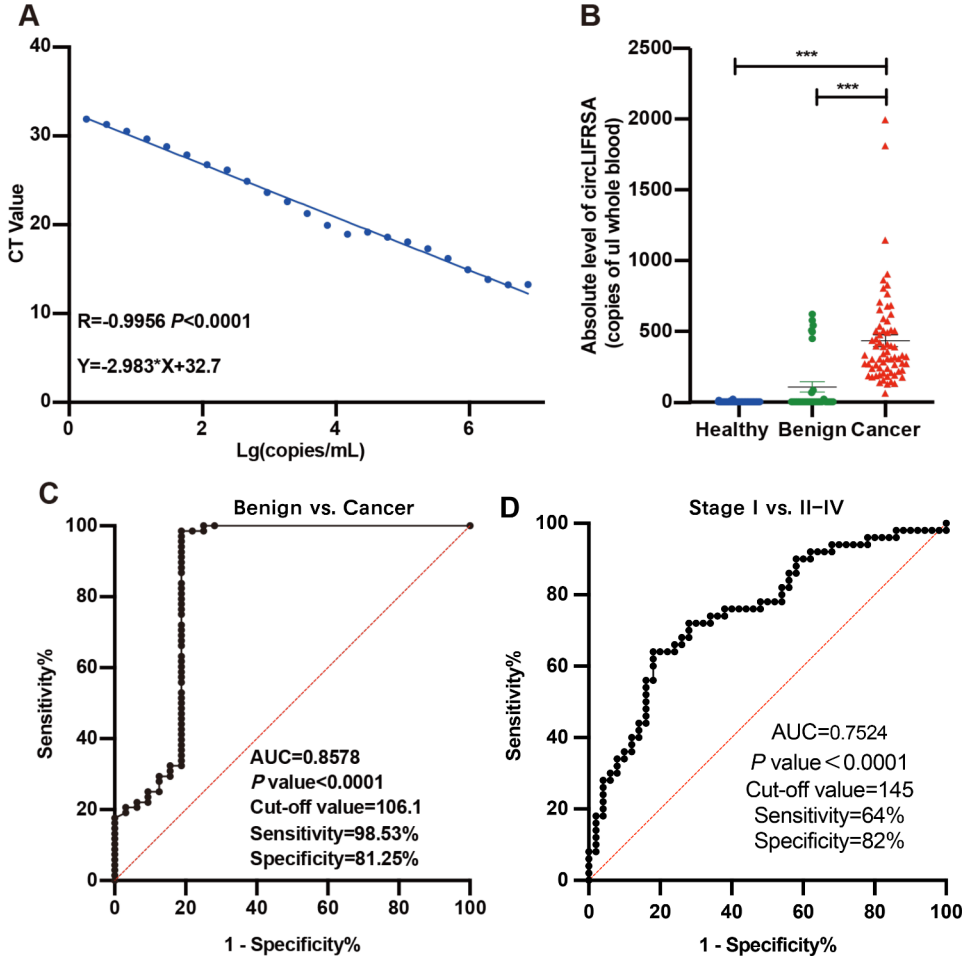

Fig. 3 CircLIFRSA serves as an early diagnostic biomarker for lung cancer. (**A**) The standard curve was used in absolute quantitation. (**B**) The expression levels of circLIFRSA in whole blood of healthy people ($n=49$), benign lung disease ($n=30$), and NSCLC ($n=60$) were detected by RT-qPCR. (**C**) ROC curve of circLIFRSA distinguishing benign lung disease from cancer patients. (**D**) ROC curve of circLIFRSA distinguishing early stage I from other stages (II-IV) in NSCLC patients.*** $P<0.001$

apoptosis compared to the control group. In addition, circLIFRSA was found to partially rescue the inhibitory effect of miR-1305 on apoptosis (Fig. 6C). However, it was observed that neither miR-1305 alone nor the simultaneous overexpression of circLIFRSA and miR-1305 significantly affected cell cycle progression (Additional file 1, Figure S5). These findings suggest that circLIFRSA suppresses malignant cellular phenotypes by sequestering miR-1305.

CircLIFRSA/miR-1305/PTEN regulatory axis modulates AKT phosphorylation

To identify potential target genes of miR-1305, we utilized a bioinformatics tool to predict candidates with complementary sequences to miR-1305 (miRbase, https://www.mirbase.org). Among the top 14 candidates selected for batch gene expression analysis at ACLBI (https://www.aclbi.com/static/index.htmL), *PTEN*, *TP53BP1*, and *SPOP* exhibited low expression in NSCLC (Fig. 7A). Considering that miRNAs typically exert a negative regulatory effect on their target genes, we transfected miR-1305 into NSCLC cells and assessed the expression levels of *PTEN*, *TP53BP1*, and *SPOP*. Notably, *PTEN* demonstrated the most significant downregulation among the four candidates (Fig. 7B). Subsequently, we predicted the potential binding sites between miR-1305 and the 3' untranslated region (3'UTR) of *PTEN* using SnapGene (https://www.snapgene.com) (Fig. 7C). A dual-luciferase activity assay confirmed the direct targeting of *PTEN* 3'UTR by miR-1305 (Fig. 7D), thereby implicating the circLIFRSA/miR-1305/PTEN regulatory axis in the malignant processes of NSCLC.

To elucidate the downstream signaling cascade associated with the circLIFRSA/miR-1305/PTEN axis, we focused on the AKT signaling effectors downstream of PTEN. Western blot analyses indicated that circLIFRSA overexpression led to an upregulation of PTEN and total AKT (tAKT), accompanied by a downregulation of

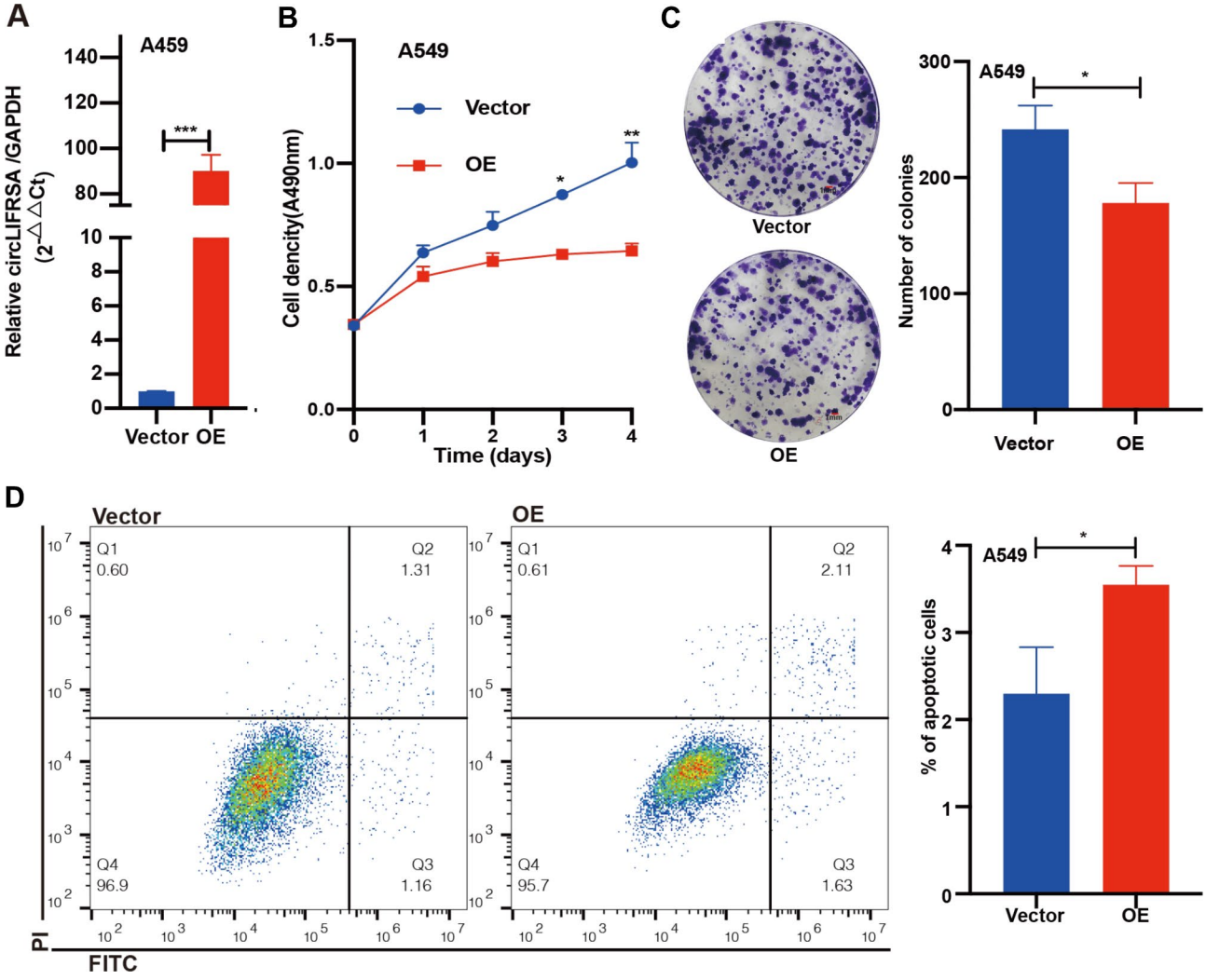

Fig. 4 CircLIFRSA exhibits inhibitory effects on the malignant processes of NSCLC cells. (**A**) Overexpression of circLIFRSA in A549 cells. (**B**) Effect of circLIFRSA overexpression on A549 cell growth by MTT assay. (**C**) Effect of circLIFRSA overexpression on A549 cell proliferation by colony formation assay. (**D**) Effect of circLIFRSA overexpression on A549 cell apoptosis by flow cytometry. * $P < 0.05$, ** $P < 0.01$, *** $P < 0.001$

phosphorylated AKT (pAKT) (Fig. 7E).In contrast, circLIFRSA knockdown resulted in decreased PTEN levels and increased pAKT levels, with no significant change in tAKT levels (Fig. 7F). Notably, treatment with miR-1305 mimics resulted in reduced PTEN expression alongside elevated pAKT levels (Fig. 7G). Furthermore, co-overexpression of circLIFRSA and miR-1305 demonstrated that circLIFRSA attenuated the inhibitory effect of miR-1305 on PTEN expression (Fig. 7H). Collectively, these finding suggest that the circLIFRSA/miR-1305/PTEN axis plays a regulatory role in AKT phosphorylation, thereby influencing the malignant cellular processes (Fig. 7I).

Discussion

While the splicing efficiency of linear RNA is generally superior to that of reverse splicing across most endogenous loci [22], circRNA exhibits enhanced stability and rapid turnover kinetics compared to linear transcripts, which facilitates its substantial accumulation in tissues [23]. This study has identified a novel circRNA associated with NSCLC, derived from LIFRSA, and established a correlation between circLIFRSA and lung cancer. CircLIFRSA is a circular RNA formed through reverse splicing between exon 2 and exon 19 of LIFRSA, resulting in a closed circular RNA molecule. Comprehensive stability assessments, utilizing actinomycin D assays, indicated that circLIFRSA possesses a significantly longer half-life than mLIFRSA, highlighting its potential as a robust biomarker.

The stability of biomarkers is crucial for liquid biopsy applications aimed at the early detection of cancer. CircRNA has emerged as a promising avenue for biomarker discovery due to its high conservation [24], tissue specificity [25], temporal specificity [26], and high

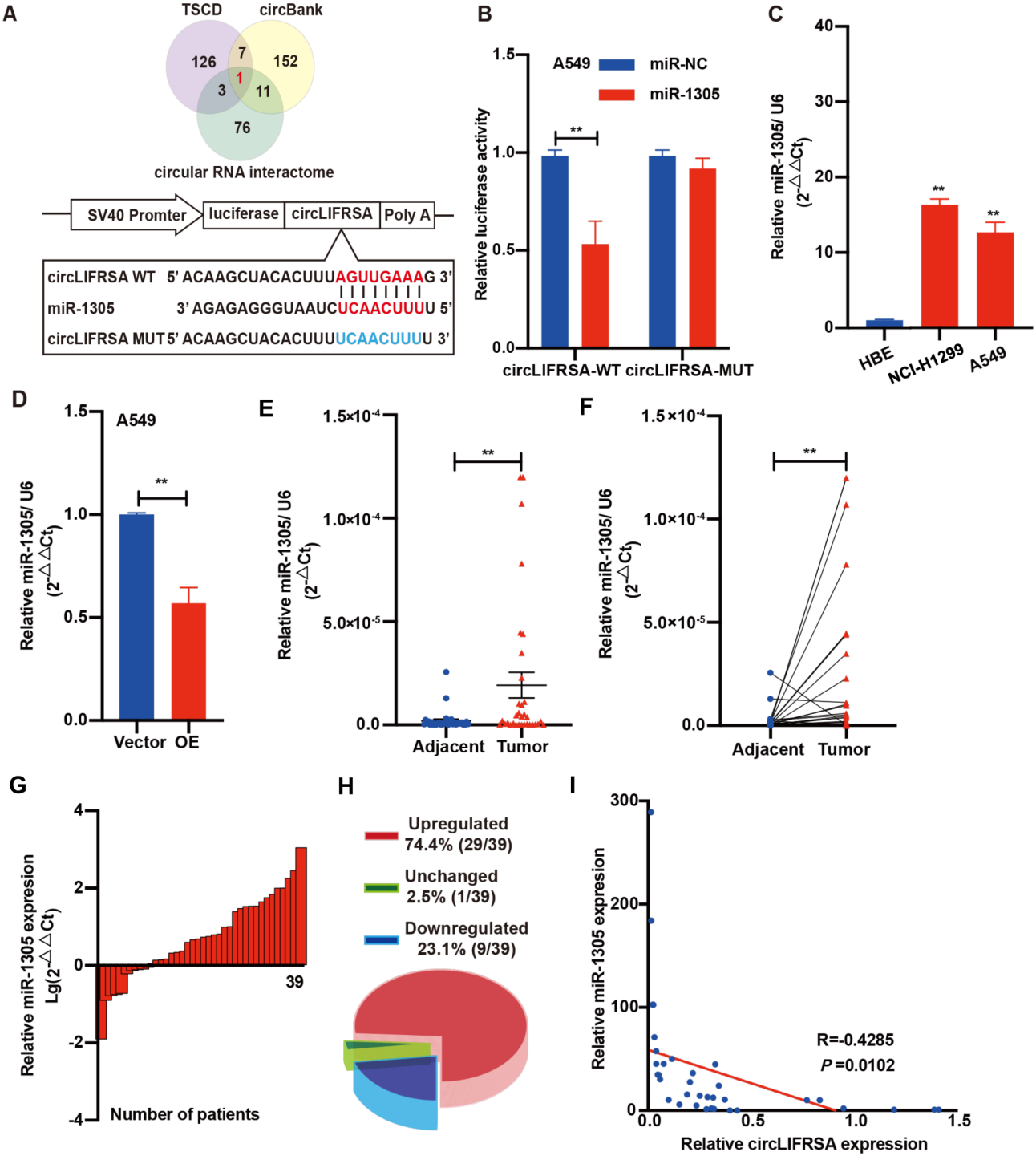

Fig. 5 CircLIFRSA interacts and negatively correlates with miR-1305. (**A**) MiR-1305 was predicted to interact with circLIFRSA through bioinformatic analysis. (**B**) MiR-1305 binds with wild-type (WT) circLIFRSA via core miRNA recognition element, but not mutated (MUT) circLIFRSA. (**C**) MiR-1305 was highly expressed in NSCLC cells. (**D**) MiR-1305 was downregulated upon circLIFRSA overexpression. (**E-H**) MiR-1305 was highly expressed in tumor tissues compared to adjacent tissues in patients with NSCLC. (**I**) CircLIFRSA was negatively correlated with miR-1305 in patients with NSCLC. ** $P < 0.01$

stability [27]. For instance, circGSK3β demonstrated consistent and elevated expression in the plasma of patients diagnosed with esophageal squamous cell carcinoma (ESCC), achieving an AUC of 0.782 for ESCC diagnosis and 0.793 for early ESCC diagnosis [28]. Conversely, circSATB2 exhibited consistent and elevated expression levels in exosomes derived from lung cancer patients, with an AUC of 0.685 for differentiating

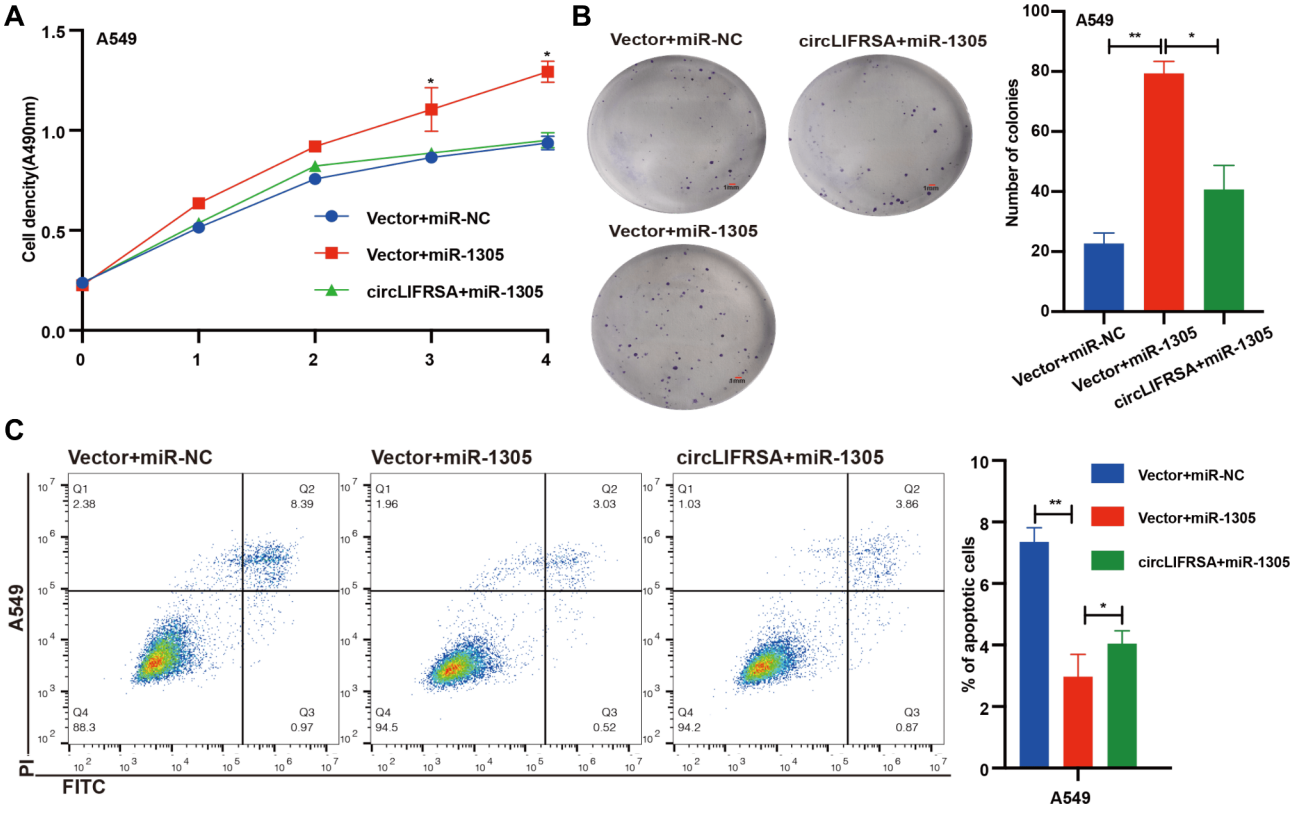

Fig. 6 CircLIFRSA suppresses the malignant processes by regulating miR-1305. (**A**) CircLIFRSA rescued miR-1305-mediated promotion of growth in A549 cells. (**B**) CircLIFRSA rescued miR-1305-mediated promotion of proliferation in A549 cells. (**C**) CircLIFRSA rescued miR-1305-mediated suppression of apoptosis in A549 cells. * $P<0.05$, ** $P<0.01$

between metastatic and non-metastatic lung cancer [29]. Additionally, circCDYL2 is significantly upregulated in trastuzumab-resistant breast cancer (BC), particularly in the HER2+subtype, where lower levels of circCDYL2 correlate with prolonged disease-free survival and overall survival compared to patients with higher levels. Consequently, circCDYL2 presents as a promising biomarker for identifying trastuzumab resistance in HER2+BC patients [30]. In the present work, circLIFRSA was found to have low expression in NSCLC tissues but was highly expressed in whole blood. This observation suggests that circLIFRSA may be actively transported from cancer cells into peripheral blood through specific mechanisms, such as exosomal transmission. Likewise, circLPAR1 showed low expression in colon cancer cells and tissues, yet exhibited high expression in plasma exosomes, with further analysis confirming its active packaging into exosomes and release from cancer cells. This indicates that circLPAR1 can be detected in plasma exosomes during the disease progression of colon cancer [31]. Therefore, the elevated expression of circLIFRSA in whole blood may result from the active efflux of cancer cells, closely associated with NSCLC development. Notably, the AUC for circLIFRSA in distinguishing benign lung diseases from NSCLC reached 0.8578. Taken together, these findings suggest that circLIFRSA is stable in peripheral blood and may serve as a promising biomarker for liquid biopsy in NSCLC diagnosis. Furthermore, the efflux of tumor suppressor molecules from cancer cells may represent a novel strategy for targeted therapy, offering new insight into translational research. However, to enhance the reliability of circLIFRSA's potential clinical application in cancer diagnosis, it is essential to address limitations related to larger sample size, comprehensive subgroup analyses, and the need for further validation in prospective cohorts.

CircRNAs, which are stable and detectable in biological fluids, present significant potential as biomarkers for innovative diagnostic and prognostic methodologies due to their correlation with various clinicopathological characteristics [32]. Nonetheless, the majority of existing studies on circRNAs as biomarkers, including our research, has primarily engaged in limited discovery verification. There is a notable deficiency of prospective cohort studies and clinical trials in this area [33]. Consequently, substantial progress is required to translate circRNA detection into actionable clinical decisions.

The relationships between circRNA expression and clinicopathological characteristics frequently suggest their influence on cellular phenotypes and underlying

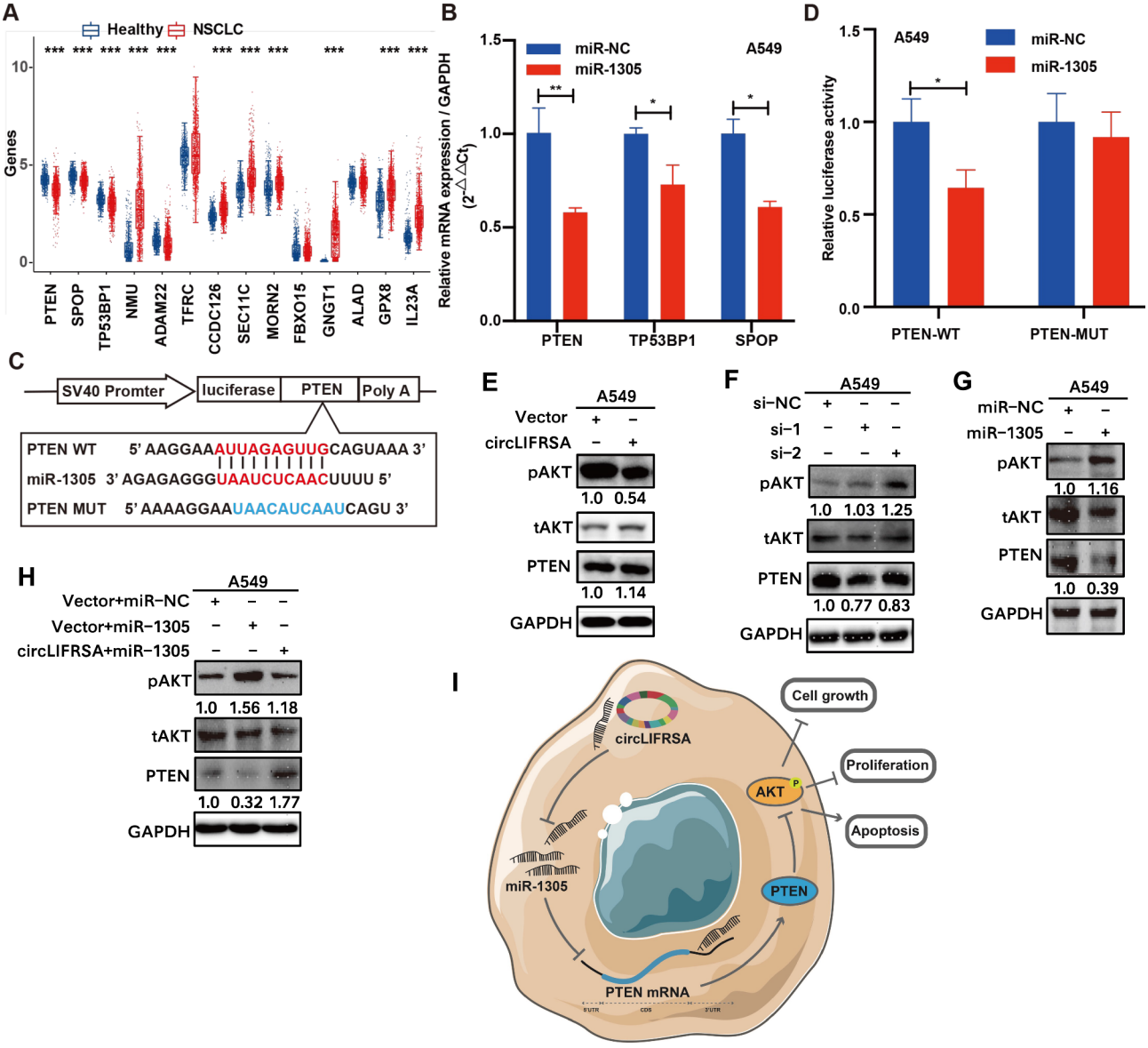

Fig. 7 CircLIFRSA/miR-1305/PTEN regulatory axis modulates AKT phosphorylation. (**A**) The expression levels of 14 candidate genes between healthy people and NSCLC patients via ALCBI. (**B**) *PTEN* showed the most significant decrease among the three selected candidate genes upon miR-1305 overexpression. (**C**) MiR-1305 was predicted to bind with the 3′-UTR of *PTEN*. (**D**) MiR-1305 could bind with the wild-type *PTEN* in A549 cells. (**E**) PTEN was upregulated and pAKT was downregulated upon circLIFRSA overexpression in A549 cells. (**F**) PTEN was downregulated and pAKT was upregulated upon circLIFRSA knockdown in A549 cells. (**G**) PTEN was downregulated and pAKT was upregulated upon miR-1305 overexpression in A549 cells. (**H**) CircLIFRSA rescued miR-1305-mediated inhibition of PTEN and pAKT in A549 cells. (**I**) Working model of circLIFRSA/miR-1305/PTEN axis on AKT phosphorylation and attenuation of malignant cellular processes. * $P < 0.05$, ** $P < 0.01$, *** $P < 0.001$

molecular mechanisms. For example, hsa_circ_0002577, which is upregulated and correlated with the TNM stage of endometrial cancer, has been shown to promote tumor growth and metastasis. Experimental studies conducted both in vitro and in vivo have demonstrated its function as a sponge for miR-625-5p, resulting in enhanced expression of IGF1R and subsequent activation of the AKT pathway [34]. In the context of triple-negative breast cancer (TNBC), hsa_circ_0000199 is significantly overexpressed and associated with tumor size, TNM stage, and Ki-67 levels. Mechanically, it acts as a sponge for miR-613 and miR-206, thereby activating the PI3K/AKT/mTOR signaling pathway, which facilitates cell proliferation, migration, invasion, and contributes to resistance to chemotherapy [35]. In patients with BC, hsa_circ_001569 is associated with lymph node metastasis and pathological type, serving as an independent prognostic factor for the 5-year overall survival rate. Enrichment analyses indicate that hsa_circ_001569 likely modulates cellular functions via the PI3K/AKT

pathway [36]. CircHIPK3, which is elevated in BC and linked to patient prognosis, promotes BC cell proliferation, migration, invasion, and tumor growth through the miR-193a/HMGB1/PI3K/AKT pathway [37]. In hepatocellular carcinoma (HCC), circIGF1R is upregulated and correlated with tumor size, playing a critical role in cellular processes. The knockdown of circIGF1R significantly inhibits cell proliferation, induces apoptosis, and causes G0/G1 cell cycle arrest through AKT activation [38]. In our study, circLIFRSA's associations with tumor size ($P=0.0381$), tumor count ($P=0.0438$), differentiation grade ($P=0.005$), and pathological type ($P=0.0144$) indicate its potential function as a tumor suppressor in NSCLC. Gain-of-function experiments were performed in NSCLC cells to clarify the impact of circLIFRSA on malignant phenotypes. The findings revealed that circLIFRSA inhibits cell growth and proliferation while inducing apoptosis, without affecting cell cycle progression.

The subcellular localization of circRNAs significantly influences their functional modalities and mechanisms, which are contingent upon their specific intracellular distribution. For example, circACTN4 predominantly sequesters miR-424-5p in the cytoplasm, functioning as a miRNA sponge that subsequently enhances the expression of Yes-associated protein 1 (YAP1). In the nuclear compartment, circACTN4 facilitates the recruitment of Y-box binding protein 1 (YBX1), thereby initiating the transcription of Frizzled-7 (FZD7) [5]. Given that circLIFRSA is primarily localized in the cytoplasm, we hypothesized that its functional role is predominantly mediated through the ceRNA mechanism. The predicted interaction between circLIFRSA and miR-1305 was substantiated by dual luciferase reporter assays. Interestingly, miR-1305, which is highly expressed and associated with poor prognosis in LUAD patients, exhibits an antagonistic role relative to circLIFRSA. Analysis of a limited clinical cohort ($n=39$) revealed a negative correlation between the expression levels of circLIFRSA and miR-1305.

PTEN, a well-established tumor suppressor, inhibits AKT phosphorylation [39]. The loss of function of tumor suppressor is frequently observed in NSCLC [40]. CircRNAs may play a role in modulating the AKT signaling pathway. In NSCLC, circGFRA1 is found to be highly expressed in tumor tissues and acts as a sponge for miR-188-3p, leading to the upregulation of PI3K and subsequent activation of the PI3K/AKT pathway, thereby promoting cell proliferation [41]. In addition, circRNA_100876 [42] and hsa_circ_0018818 [43] have been implicated in the regulation of malignant processes through modulation of AKT signaling in NSCLC. In our work, we demonstrated that miR-1305 negatively regulates PTEN, which in turn activates AKT phosphorylation. Interestingly, circLIFRSA functions as a tumor suppressor by upregulating PTEN and counteracting the downregulation of PTEN induced by miR-1305. In essence, circLIFRSA competes with PTEN for binding to miR-1305, leading to the upregulation of PTEN, inhibition of AKT phosphorylation, and ultimately the suppression of malignant phenotypes in NSCLC.

In summary, we have identified circLIFRSA as a novel tumor suppressor, elucidating its role in attenuating malignant processes through the circLIFRSA/miR-1305/PTEN axis and the regulation of AKT phosphorylation in NSCLC. Furthermore, the elevated expression of circLIFRSA in peripheral blood presents promising diagnostic potential for differentiating NSCLC from benign lung disease, positioning it as a prospective biomarker and therapeutic target for the management of NSCLC.

Supplementary Information

The online version contains supplementary material available at https://doi.org/10.1186/s12943-024-02120-w.

Supplementary Material 1: Figure S1 Flowchart of analysis for NSCLC tissue samples.Figure S2 Flowchart of ROC analysis for blood samples.Figure S3 CircLIFRSA does not affect cell cycle in A549 cells.Figure S4 MiR-1305 predicts poor prognosis in LUAD.Figure S5 MiR-1305 alone, and circLIFRSA/miR-1305 combination have no effects on cell cycle in NSCLC.

Supplementary Material 2: Table S1 RNA oligonucleotide sequences.Table S2 Primer sequences.Table S3 Demographics of healthy controls and patients with benign lung disease.

Acknowledgements

We thank the core facility platform of Ningbo University Health Science Center for its technical support.

Author contributions

Z.G. and M.J. developed the concepts and designed the study. M.J., H.B., S.F., C.Z. and W.S. performed the experiments. M.J. drafted the manuscript. Z.G. and M.J. discussed and revised the manuscript.

Funding

This work was supported by research grants from the Major Project for Science and Technology Innovation 2025 of Ningbo (2019B10037), the Ningbo Clinical Research Center for Respiratory Diseases (2022L004), and the K.C. Wong Magna Fund at Ningbo University.

Data availability

No datasets were generated or analysed during the current study.

Declarations

Ethics approval and consent to participate

The study was approved by the Medical Research Ethics Committee of Ningbo University (Approval No.: NBU-2021-032), and all participants provided written informed consent. All methods were performed in accordance with relevant guidelines and local regulations.

Consent for publication

Not applicable.

Competing interests

The authors declare no competing interests.

Received: 18 April 2024 / Accepted: 10 September 2024
Published online: 28 September 2024

References

1. Siegel RL, Miller KD, Fuchs HE, Jemal A. Cancer statistics, 2022. CA Cancer J Clin. 2022;72:7–33.
2. Molina JR, Yang P, Cassivi SD, Schild SE, Adjei AA. Non-small cell lung cancer: epidemiology, risk factors, treatment, and survivorship. Mayo Clin Proc. 2008;83:584–94.
3. Thai AA, Solomon BJ, Sequist LV, Gainor JF, Heist RS. Lung cancer. Lancet. 2021;398:535–54.
4. Xu Y, Leng K, Yao Y, Kang P, Liao G, Han Y, Shi G, Ji D, Huang P, Zheng W, et al. A circular RNA, cholangiocarcinoma-associated circular RNA 1, contributes to cholangiocarcinoma progression, induces angiogenesis, and disrupts vascular endothelial barriers. Hepatology. 2021;73:1419–35.
5. Chen Q, Wang H, Li Z, Li F, Liang L, Zou Y, Shen H, Li J, Xia Y, Cheng Z, et al. Circular RNA ACTN4 promotes intrahepatic cholangiocarcinoma progression by recruiting YBX1 to initiate FZD7 transcription. J Hepatol. 2022;76:135–47.
6. Cheng Z, Yu C, Cui S, Wang H, Jin H, Wang C, Li B, Qin M, Yang C, He J, et al. circTP63 functions as a ceRNA to promote lung squamous cell carcinoma progression by upregulating FOXM1. Nat Commun. 2019;10:3200.
7. Li Z, Huang C, Bao C, Chen L, Lin M, Wang X, Zhong G, Yu B, Hu W, Dai L, et al. Exon-intron circular RNAs regulate transcription in the nucleus. Nat Struct Mol Biol. 2015;22:256–64.
8. Zhang Y, Zhang XO, Chen T, Xiang JF, Yin QF, Xing YH, Zhu S, Yang L, Chen LL. Circular intronic long noncoding RNAs. Mol Cell. 2013;51:792–806.
9. Xu J, Wan Z, Tang M, Lin Z, Jiang S, Ji L, Gorshkov K, Mao Q, Xia S, Cen D, et al. N(6)-methyladenosine-modified CircRNA-SORE sustains sorafenib resistance in hepatocellular carcinoma by regulating β-catenin signaling. Mol Cancer. 2020;19:163.
10. Li B, Zhu L, Lu C, Wang C, Wang H, Jin H, Ma X, Cheng Z, Yu C, Wang S, et al. circNDUFB2 inhibits non-small cell lung cancer progression via destabilizing IGF2BPs and activating anti-tumor immunity. Nat Commun. 2021;12:295.
11. Du WW, Yang W, Liu E, Yang Z, Dhaliwal P, Yang BB. Foxo3 circular RNA retards cell cycle progression via forming ternary complexes with p21 and CDK2. Nucleic Acids Res. 2016;44:2846–58.
12. Chen Y, Lin Y, Shu Y, He J, Gao W. Interaction between N(6)-methyladenosine (m(6)A) modification and noncoding RNAs in cancer. Mol Cancer. 2020;19:94.
13. Wang L, Tong X, Zhou Z, Wang S, Lei Z, Zhang T, Liu Z, Zeng Y, Li C, Zhao J, et al. Circular RNA hsa_circ_0008305 (circPTK2) inhibits TGF-β-induced epithelial-mesenchymal transition and metastasis by controlling TIF1γ in non-small cell lung cancer. Mol Cancer. 2018;17:140.
14. Fruman DA, Chiu H, Hopkins BD, Bagrodia S, Cantley LC, Abraham RT. The PI3K pathway in human disease. Cell. 2017;170:605–35.
15. Fruman DA, Rommel C. PI3K and cancer: lessons, challenges and opportunities. Nat Rev Drug Discov. 2014;13:140–56.
16. Shi Y, Fang N, Li Y, Guo Z, Jiang W, He Y, Ma Z, Chen Y. Circular RNA LPAR3 sponges microRNA-198 to facilitate esophageal cancer migration, invasion, and metastasis. Cancer Sci. 2020;111:2824–36.
17. He Y, Mingyan E, Wang C, Liu G, Shi M, Liu S. CircVRK1 regulates tumor progression and radioresistance in esophageal squamous cell carcinoma by regulating miR-624-3p/PTEN/PI3K/AKT signaling pathway. Int J Biol Macromol. 2019;125:116–23.
18. Gkountakos A, Sartori G, Falcone I, Piro G, Ciuffreda L, Carbone C, Tortora G, Scarpa A, Bria E, Milella M et al. PTEN in lung cancer: dealing with the problem, building on new knowledge and turning the game around. Cancers (Basel). 2019;11:1141.
19. Yu J, Xu QG, Wang ZG, Yang Y, Zhang L, Ma JZ, Sun SH, Yang F, Zhou WP. Circular RNA cSMARCA5 inhibits growth and metastasis in hepatocellular carcinoma. J Hepatol. 2018;68:1214–27.
20. Pan J, Fang S, Tian H, Zhou C, Zhao X, Tian H, He J, Shen W, Meng X, Jin X, Gong Z. lncRNA JPX/miR-33a-5p/Twist1 axis regulates tumorigenesis and metastasis of lung cancer by activating Wnt/β-catenin signaling. Mol Cancer. 2020;19:9.
21. Huang H, Weng H, Sun W, Qin X, Shi H, Wu H, Zhao BS, Mesquita A, Liu C, Yuan CL, et al. Recognition of RNA N(6)-methyladenosine by IGF2BP proteins enhances mRNA stability and translation. Nat Cell Biol. 2018;20:285–95.
22. Zhang Y, Xue W, Li X, Zhang J, Chen S, Zhang JL, Yang L, Chen LL. The biogenesis of nascent circular RNAs. Cell Rep. 2016;15:611–24.
23. Chen LL. The expanding regulatory mechanisms and cellular functions of circular RNAs. Nat Rev Mol Cell Biol 2020.
24. Shang BQ, Li ML, Quan HY, Hou PF, Li ZW, Chu SF, Zheng JN, Bai J. Functional roles of circular RNAs during epithelial-to-mesenchymal transition. Mol Cancer. 2019;18:138.
25. Lorenzi L, Chiu HS, Avila Cobos F, Gross S, Volders PJ, Cannoodt R, Nuytens J, Vanderheyden K, Anckaert J, Lefever S, et al. The RNA Atlas expands the catalog of human non-coding RNAs. Nat Biotechnol. 2021;39:1453–65.
26. Ruan H, Xiang Y, Ko J, Li S, Jing Y, Zhu X, Ye Y, Zhang Z, Mills T, Feng J, et al. Comprehensive characterization of circular RNAs in ~ 1000 human cancer cell lines. Genome Med. 2019;11:55.
27. Patop IL, Wüst S, Kadener S. Past, present, and future of circRNAs. EMBO J. 2019;38:e100836.
28. Hu X, Wu D, He X, Zhao H, He Z, Lin J, Wang K, Wang W, Pan Z, Lin H, Wang M. circGSK3beta promotes metastasis in esophageal squamous cell carcinoma by augmenting beta-catenin signaling. Mol Cancer. 2019;18:160.
29. Zhang N, Nan A, Chen L, Li X, Jia Y, Qiu M, Dai X, Zhou H, Zhu J, Zhang H, Jiang Y. Circular RNA circSATB2 promotes progression of non-small cell lung cancer cells. Mol Cancer. 2020;19:101.
30. Ling Y, Liang G, Lin Q, Fang X, Luo Q, Cen Y, Mehrpour M, Hamai A, Liu Z, Shi Y, et al. circCDYL2 promotes trastuzumab resistance via sustaining HER2 downstream signaling in breast cancer. Mol Cancer. 2022;21:8.
31. Zheng R, Zhang K, Tan S, Gao F, Zhang Y, Xu W, Wang H, Gu D, Zhu L, Li S, et al. Exosomal circLPAR1 functions in colorectal cancer diagnosis and tumorigenesis through suppressing BRD4 via METTL3-eIF3h interaction. Mol Cancer. 2022;21:49.
32. Zhang HD, Jiang LH, Sun DW, Hou JC, Ji ZL. CircRNA: a novel type of biomarker for cancer. Breast Cancer. 2018;25:1–7.
33. Kristensen LS, Jakobsen T, Hager H, Kjems J. The emerging roles of circRNAs in cancer and oncology. Nat Rev Clin Oncol. 2022;19:188–206.
34. Wang Y, Yin L, Sun X. CircRNA hsa_circ_0002577 accelerates endometrial cancer progression through activating IGF1R/PI3K/Akt pathway. J Exp Clin Cancer Res. 2020;39:169.
35. Li H, Xu W, Xia Z, Liu W, Pan G, Ding J, Li J, Wang J, Xie X, Jiang D. Hsa_circ_0000199 facilitates chemo-tolerance of triple-negative breast cancer by interfering with miR-206/613-led PI3K/Akt/mTOR signaling. Aging. 2021;13:4522–51.
36. Xu JH, Wang Y, Xu D. Hsa_circ_001569 is an unfavorable prognostic factor and promotes cell proliferation and metastasis by modulating PI3K-AKT pathway in breast cancer. Cancer Biomark. 2019;25:193–201.
37. Chen ZG, Zhao HJ, Lin L, Liu JB, Bai JZ, Wang GS. Circular RNA CirCHIPK3 promotes cell proliferation and invasion of breast cancer by sponging miR-193a/HMGB1/PI3K/AKT axis. Thorac Cancer. 2020;11:2660–71.
38. Fu HW, Lin X, Zhu YX, Lan X, Kuang Y, Wang YZ, Ke ZG, Yuan T, Chen P. CircIGF1R has pro-proliferative and anti-apoptotic effects in HCC by activating the PI3K/AKT pathway. Gene. 2019;716:144031.
39. Chai C, Wu HH, Abuetabh Y, Sergi C, Leng R. Regulation of the tumor suppressor PTEN in triple-negative breast cancer. Cancer Lett. 2022;527:41–8.
40. Álvarez-Garcia V, Tawil Y, Wise HM, Leslie NR. Mechanisms of PTEN loss in cancer: it's all about diversity. Semin Cancer Biol. 2019;59:66–79.
41. Yao J, Xu G, Zhu L, Zheng H. circGFRA1 enhances NSCLC progression by sponging miR-188-3p. Onco Targets Ther. 2020;13:549–58.
42. Song J, Shi W, Gao Z, Liu X, Wang W. Downregulation of circRNA_100876 inhibited progression of NSCLC in vitro via targeting miR-636. Technol Cancer Res Treat. 2020;19:1533033820951817.
43. Xu X, Zhou X, Gao C, Cui Y. Hsa_circ_0018818 knockdown suppresses tumorigenesis in non-small cell lung cancer by sponging miR-767-3p. Aging. 2020;12:7774–85.

Publisher's note